

Solid tungsten Divertor-III for ASDEX Upgrade and contributions to ITER

A. Herrmann, H. Greuner, N. Jaksic, M. Balden, A. Kallenbach, K. Krieger, P. de Marne, V. Rohde, A. Scarabosio, G. Schall, ASDEX Upgrade team

Max-Planck-Institut für Plasmaphysik, Boltzmannstr. 2, D-85748 Garching, Germany

E-mail: albrecht.herrmann@ipp.mpg.de

Abstract ASDEX Upgrade became a full tungsten experiment in 2007 by coating its graphite plasma facing components with tungsten. In 2013 a redesigned solid tungsten divertor, Div-III, was installed and came into operation in 2014. The redesign of the outer divertor geometry provided the opportunity to increase the pumping efficiency in the lower divertor by increasing the gap between divertor and vessel. In parallel, a by-pass was installed into the cryo-pump in the divertor region allowing adapting the pumping speed to the required edge density.

Safe divertor operation and heat removal becomes more and more significant for future fusion devices. This requires developing ‘tools’ for divertor heat load control and to optimize the divertor design. The new divertor manipulator, DIM-II, allows retracting a relevant part of the outer divertor into a target exchange box without venting ASDEX Upgrade. Different front-ends can be installed and exposed to the plasma. At present, front-ends for probe exposition, gas puffing, electrical probes and actively cooled prototype targets are under construction.

The installation of solid tungsten, the control of the pumping speed and the flexibility for testing divertor modifications on a weekly base is a unique feature of ASDEX Upgrade and offers together with the extended set of diagnostics the possibility to investigate dedicated questions for a future divertor design.

1. Introduction

The mid-size tokamak ASDEX Upgrade in Garching has been operated for more than 20 years and 30 000 discharges. During this period the operation capabilities have been permanently improved according to the physics research program that focuses on the development of commercial fusion reactors. Major improvements were the installation of a second neutral beam injector and the upgrade of the electron cyclotron heating system. The need to operate a divertor within a technological acceptable heat load drives the divertor evolution. This way the open divertor Div-I of ASDEX Upgrade was in a first step replaced by an optimized Lyre-shaped closed divertor – Div-IIa. Later divertor modifications kept the advantage of a vertical target plate for divertor recycling and radiation but were more flexible with respect to allowed magnetic configurations [1].

In 2007 ASDEX Upgrade became a full tungsten experiment [2]. At this time all plasma facing graphite tiles were coated with tungsten. The outer divertor, the region with the strongest erosion was in a first step coated with 200 μm tungsten. This thick coating delaminated after discharges with a high heat load due to the induced thermal stress. The delaminated tungsten flakes caused disruptions. As a consequence the thick coating was replaced by a thin 10 μm coating. [3]

The most recent step in the divertor improvement done in 2013 was the installation of a solid tungsten divertor made from powder metallurgy (PM) tungsten [4]. The new Div-III expands the operational domain of ASDEX Upgrade and it overcomes the problem of either risking a delamination of thick tungsten coatings or a frequent exchange of target plates with thin layers. In addition, Div-III allows physics investigations such as erosion of tungsten and deuterium retention in solid tungsten. Further features realized with the new design are an improved pumping speed in the divertor and the possibility for adaptable divertor instrumentation and investigation.

This paper reports on the design and the operation range in section 2. Section 3 summarizes the experiences of one campaign of operation. Contributions to ITER scenario development and divertor design are discussed in section 4. Finally a summary is given.

2. Divertor design and operation range

ASDEX Upgrade was designed for operation with pulsed discharges of up to 10 s plasma current plateau phase. The technical systems such as the power supply with fly-wheel

generators, the cooling of the toroidal and vertical field coils, are designed according to this parameter. Consequently, the divertors Div-I to Div-II_d were developed as adiabatically loaded divertors with an energy absorption capacity of about 50 MJ/discharge that corresponds to the available heating power of 25 MW in maximum.

Div-III is designed also as an adiabatically loaded divertor. Based on the successful prototype test during the 2010/11 experimental campaigns [5] the basic requirements for the new solid tungsten divertor Div-III were defined:

- i. It should have at least the same energy and heat load receiving capability as a graphite divertor without tungsten coating.
- ii. It should keep the possibility of manual handling inside the vessel during the assembly process. This was an issue due to the much higher weight of tungsten tiles compared to the previous graphite tiles.
- iii. The redesign of the divertor should be used to increase the pumping efficiency in the divertor by increasing the conductance between the roof baffle and the cryo-pump located behind the lower outer divertor.
- iv. A possibility for reduction of the cryo-pumping speed should be possible for accessibility of high divertor neutral pressure.
- v. A relevant part of the divertor should be kept flexible with respect to tile shape, cooling and instrumentation to contribute to R&D on divertor design for future fusion reactors.

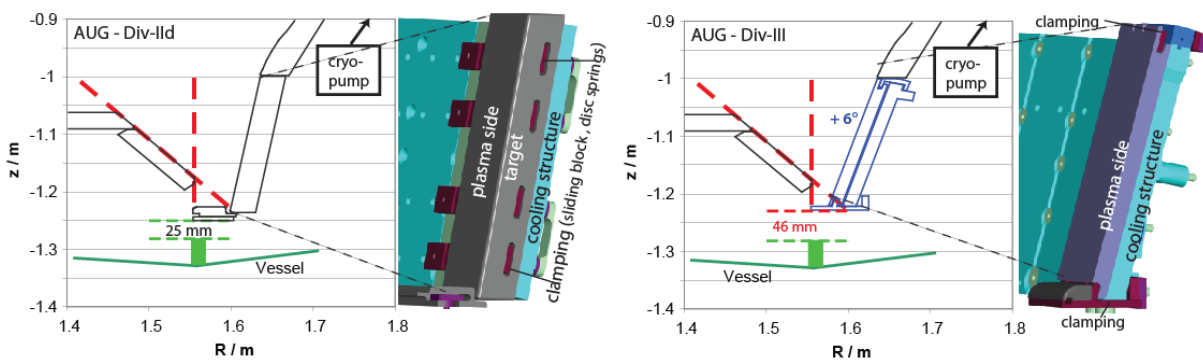


Fig. 1 shows the previous Div-II_d configuration (left) and the new Div-III geometry (right). Dashed lines mark the operation range for magnetic configurations.

Fig. 1 shows the design modifications of Div-III compared to the previous Div-II_d. Div-II_d targets consist of 30 mm thick fine grain graphite plates coated with tungsten. The graphite plates were clamped to a stainless steel cooling structure by sliding blocks, bolts and disc springs made of Inconel at the rear side of the water cooled structure. The clamping of the graphite plates had to be done before the assembly of the divertor module into the vacuum vessel. The conductance below the outer divertor is low due to the small gap between the

bottom of the divertor and the vessel. It is increased with the Div-III geometry by shortening the target and increasing the gap between the lower end of the divertor and the vessel. Simultaneously, the inclination of the target is increased by 6° to allow plasma operation with the same magnetic configurations as in Div-II d. The change of the target inclination results in a larger poloidal pitch angle but a wider field line expansion so that the increase of the peak heat load in Div-III compared to Div-II d is about 2-6% in dependence on the magnetic configuration.

The assembly procedure for Div-III is also modified compared to Div-II d considering the increased weight of the tungsten targets. First, the divertor support structure with the water cooling is mounted in the vacuum vessel. Then the tungsten target plates are clamped to the cooling structure by an upper and lower claw as shown in the exploded view of Fig. 2. The weight of a single target plate is increased by a factor 5 to about 5 kg due to the 10 fold higher density at half the thickness compared to graphite. In total, the weight increase of the divertor is about 600 kg or 1 % of the ASDEX Upgrade vacuum vessel weight.

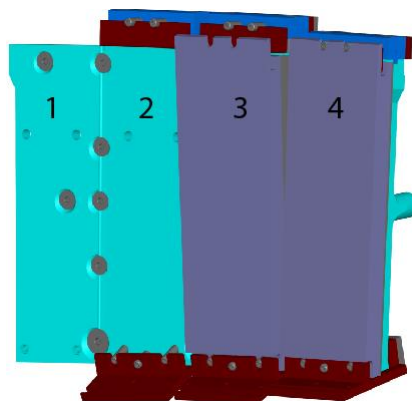


Fig. 2 Shows the assembly procedure for Div-III. (1) Pure water cooled back plate, (2) Upper and lower clamping claw mounted, (3) Solid tungsten target moved into the lower clamping claw and finally (4). The target is clamped by the upper and lower claw to the cooled back plate.

In preparation of Div-III, in 2010 two tungsten plates of 15 mm thickness compatible to the Div-II d design were installed [5] and operated for one and two operation campaigns, respectively. These tiles show deep cracks in front of the mounting rods where the material thickness is reduced to 3 mm (see Fig 1 in [5]). The new design of the clamping avoids this origin for cracks. In addition to these deep cracks a network of shallow cracks nearby to the area of maximum heat load was found. These cracks have due to the shallow depth no effect on the mechanical stiffness of the target.

The design of the final target shape and clamping for Div-III was verified by extensive finite element analysis, FEA, simulating the thermo-mechanical load [6]. After FEA design

optimization, the target including the clamping was tested in the high heat flux test facility GLADIS [7] at IPP. These tests have been performed up to a 3 fold thermal overload with respect to the design criteria [5]. The successful tested concept was realized and installed in 2013.

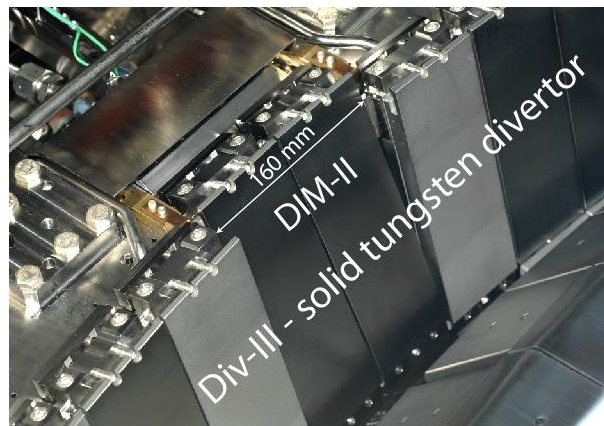


Fig. 3 Photograph of Div-III with the slightly retracted DIM-II front-end. The target tiles at the left and right of DIM-II are sand blasted to increase the emissivity for optical measurements.

In parallel to Div-III a new large divertor manipulator, DIM-II, was installed. It allows exchanging a two target wide part of the divertor including the cooling structure without venting ASDEX Upgrade. Fig. 3 shows a photograph of the realized divertor Div-III and DIM-II.

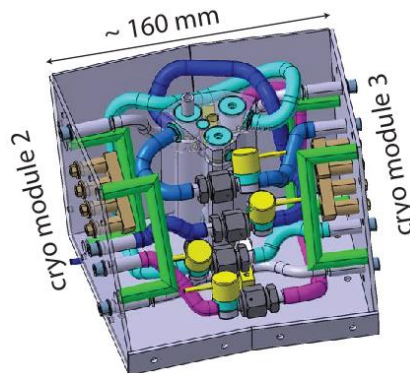


Fig. 4 CAD model of the liquid He by-pass valve consisting of 3 single valves. The by-pass valve is placed in between two cryo-panel modules. The by-pass valve is driven by pressurized He of 2.5 bar.

The opening was also used to install a liquid He valve into the cryo-pump as by-pass (Fig. 4). Due to the need to integrate the He by-pass valve into the existing cryo-pump and the limited available space, the He by-pass valve was designed and manufactured at IPP. The He by-pass valve allows operating the cryo-pump with full or 1/3 of the active panel size. The operation with full pumping speed in combination with the increased conductance reduces the density in

the scrape off layer, SOL. This increases the overlap of ASDEX Upgrade and ITER edge parameters, density and collisionality. The access to higher SOL densities is kept by the reduction of the active panel size, i.e. the pumping speed. Altogether the operational space for SOL density and collisionality at ASDEX Upgrade is extended.

3. Operation with Div-III

The new divertor Div-III was operated for over 800 plasma shots in 2014. During this campaign pulse lengths of up to 10 s and a heating energy of up to 100 MJ were achieved. Applying a maximum heating power of about 25 MW stable operation could be demonstrated at a normalized heat flux of $P_{sep}/R = 10 \text{ MW/m}$, about 2/3 of the ITER value, under partially detached conditions with a peak heat load at the target below 10 MW/m^2 [8]. Hence, the cryo by-pass valve was used for the achievement of the required high divertor neutral pressure of more than 4 Pa.

Fig. 5 shows the normalized distribution of general discharge parameters - discharge duration and plasma heating energy - for the last campaign with Div-II and the first Div-III campaign. It is obvious that the fraction of long lasting discharges and discharges with high heating energy is increased for Div-III. Safe plasma operation was achieved over the whole campaign supporting the successful design of Div-III. The large fraction of discharges with low heating energy is due to low power shots required by the experimental programme.

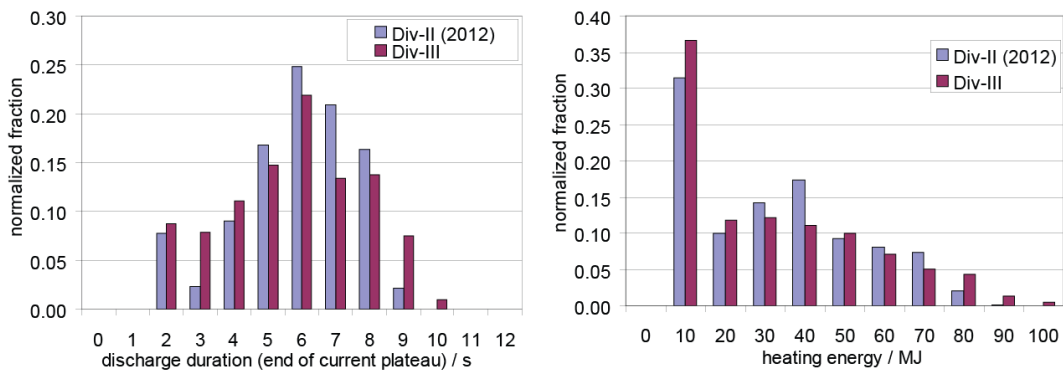


Fig. 5 Normalized distribution of the discharge duration (left) and the plasma heating energy (right) for the last campaign with Div-II and the first Div-III campaign.

During the Div-III campaign the divertor manipulator DIM-II was used to retract targets and to inspect them. Two findings are obvious as can be seen in Fig. 6. There is a different damage behaviour between the 12 targets tested in the high heat flux facility GLADIS and the targets exposed to the plasma although the number of high heat load cycles was higher for the test targets. The surface of the plasma exposed target is damaged by a network of shallow

cracks in particular in the region close to the region of highest heat load. Whereas these cracks are limited to the surface region a single crack in the centre of the target is through the whole depth. This deep crack starts at the lower edge of the target below the clamping and propagates poloidally. An in vessel inspection after venting reveals that these finding is typical for about 90% of the targets.

The origin of the shallow cracks is assumed due to temperature gradients resulting from the inhomogeneous load onto the target in combination with the operation range of the adiabatically loaded target as shown in Fig. 2 of [4]. The target temperature at the beginning of the discharge is about 20°C, i.e. tungsten is brittle. During the discharge, the surface temperature evolves up to the temperature region where tungsten becomes ductile; at more elevated temperature recrystallization starts at the surface. Typically, the bulk temperature of the tungsten target after the end of a discharge is about 300°C and will never exceed 1000°C due to the operation limits preventing recrystallization of the bulk material. Metallographic investigations of the tungsten modification were started.

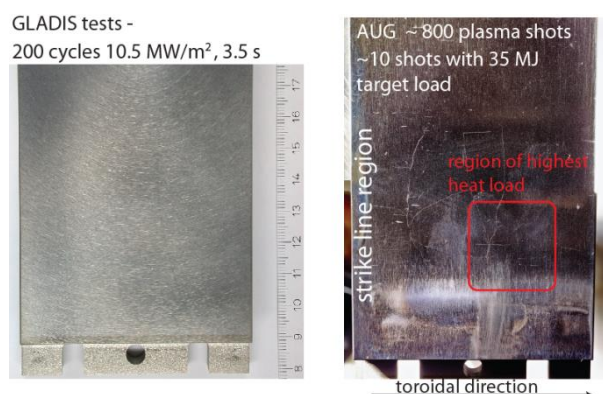


Fig. 6 Photographs of tungsten tiles taken after high heat load tests in GLADIS (left) and after one campaign of operation in ASDEX Upgrade (right).

The origin of the deep cracks is not fully understood. Deep cracks were never observed during the previous tests in ASDX Upgrade and during the high heat load test in GLADIS done with a similar clamping of the target. Loading of a pre damaged tile in GLADIS reveals that the crack propagates only if the heat load deposition area is moved towards the end of the crack. Further investigation by FEA and additional high heat flux tests with the aim of reproducing the deep cracks are scheduled. An original Div-III support structure equipped with four W tiles will be tested in GLADIS. A 15 mm thick graphite dump plate with a 15 x 80 mm² cut-out will be installed in front of the loaded target. The dump plate absorbs the heat load of the Gaussian GLADIS beam (FWHM=150 mm) and the cut-out generates a strike line like

loading with steep gradients in poloidal and toroidal direction. The test will be performed with 10 MW/m^2 heat flux at 3.5 s pulse length and 23 MW/m^2 at 0.7 s.

It should be mentioned that a deep crack in poloidal direction has neither effect on the stability of the mechanical fixing of the target nor these cracks have had an effect on the plasma performance.

The difference in cracking behaviour between GLADIS tests and ASDEX Upgrade is not fully understood yet and has to be investigated and published in a separate paper. This paper will also discuss the ASDEX Upgrade findings in the framework of published results from other groups. Cracking behaviour of solid tungsten under pulsed, ELM like, heat load is investigated and characterized in lab experiments to prepare the use of tungsten as divertor material in ITER [9, 10]. A survey of heat load and temperature of cracking is given in [11]. Experimental experience in fusion experiments is gained from the operation of a solid tungsten divertor in JET [12, 13]. This divertor is designed to minimize the effect of electromagnetic forces in contrast to the ASDEX Upgrade divertor that has to tolerate torque and forces due to disruptions due to the larger size of the targets. In addition to the thermo-mechanical load the induced forces during disruptions might play a role in producing the deep crack.

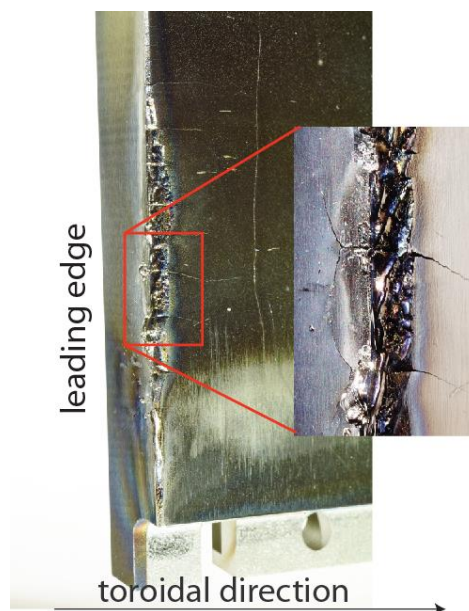


Fig. 7 Photograph of tungsten tile exposed during the 2014 campaign in ASDEX Upgrade with a protruding edge of about 1 mm exposed for more than 500 discharges. In addition to the damage at the leading edge, the target shows the deep crack and the network of shallow cracks.

Unintentionally, the effect of strongly overloaded tungsten on the plasma performance was tested by exposing leading edges resulting from a misaligned component caused by a disruption. The divertor design avoids leading edges by tilting the target tiles. The shadowing depth is -0.8 mm with 3 mm toroidal gap size. The shadow at the interface between the 16 divertor sections is adjusted during the assembly of the modules. Forces onto the divertor support structure due to eddy currents induced by disruptions were calculated in the design phase, here $dB_{\text{rad}}/dt = 20 \text{ T/s}$ and $dB_{\text{pol}}/dT = 200 \text{ T/s}$ were assumed. With this data, the clamping force is about 3 times higher than the shear force at the clamping due to the induced torque. Nevertheless during a disruption, a few divertor modules were slightly displaced. This caused leading edges of up to +1 mm resulting in a strong overload of the corresponding tungsten tile. The hot edge was detected by the video real-time divertor monitoring system [14] and results in a controlled ramp down of the discharge. After inspection of plasma parameters like plasma radiation, stored energy and tungsten concentration in the plasma core as well as the total load to the divertor tile the hot spot was accepted for further plasma operation. This finding is consistent with dedicated melting experiments in the divertor that reveals no or a weak effect onto the central plasma [15, 16]. During summer opening of ASDEX Upgrade, this tile was replaced. A photograph of the leading edge is shown in Fig. 7.

4. Contributions for ITER

The installation of solid tungsten divertor, the control of the pumping speed and the flexibility for testing divertor modifications using DIM-II offers together with the extended set of diagnostics the possibility to investigate dedicated questions for a future reactor design, such as power exhaust and divertor detachment by density and impurity control in the SOL and the divertor chamber, test of tungsten and new materials under plasma load in addition to high heat load tests, verification of geometric effects like target shadowing and castellation under shallow magnetic pitch angle, investigation of material erosion and deposition and last not least gaining experience in operation of a solid tungsten divertor under ITER like heat loads.

4.1. Divertor and SOL density control

The pumping efficiency in the lower divertor is improved by increasing the gap between the outer target and the vessel. To retain the operational range for the magnetic configurations the target was tilted further by 6° compared to Div IIb (Fig. 1). Doubling the gap size between the bottom of the divertor and the vessel has increased the conductance between cryo-pump and the divertor region by more than a factor of two. SOLPS simulations of the new divertor

predicted that the doubling of the conductance would result in an increase of the pumping efficiency of about 30% [4] in the case of low density plasmas. The pumping efficiency is defined here as the ratio of neutral fluxes in the pumping chamber and below the roof baffle. To test the prediction similarly long, low plasma density, L-mode discharges with stationary gas injection rate and neutral pressure distribution were compared. For nearly identical divertor neutral flux density (to ensure the same flow regime) the new Div-III showed a flux ratio of $\sim 0.28 \pm 0.05$ against a ratio of $\sim 0.22 \pm 0.04$ for Div-II, thus with an increment close to the predicted 30%. This improvement may seem modest but it should be compared with the maximum achievable when most of the pumping speed is switched off. In ASDEX Upgrade this is obtained by warming up the cryo-pump leading to a ~ 10 fold reduction of the nominal pumping speed, now mostly provided by a set of turbo molecular pumps. For similarly discharges with Div-II and warm cryo-pump the flux ratio only reached the value of ~ 0.33 . This limitation is attributed, as also suggested by simulations, to the gas leakages from the pump chamber back into the main chamber, both in the mid-plane and divertor regions. However, it must be said that, given the unavoidable uncertainty on the pressure measurements ($\sim 10\%$), only a statistical analysis of a large number of pulses can provide better evaluation of the pumping efficiency. This work is planned and left for future publications together with the assessment of the new operational collisionality range.

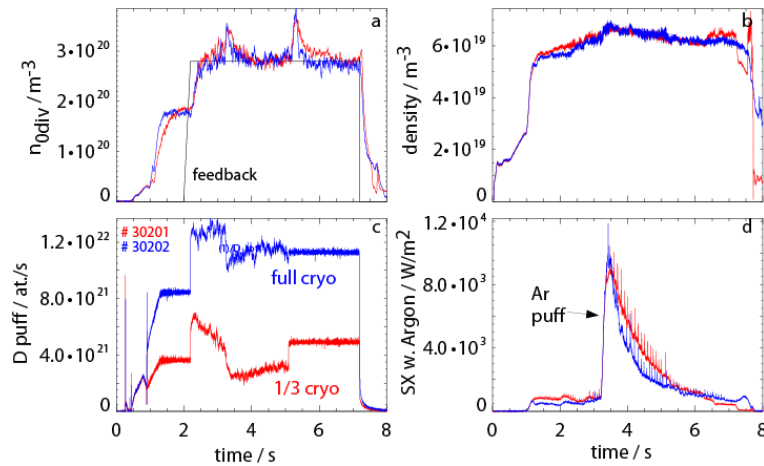


Fig. 8 Time traces comparing two discharges, with full and reduced pumping speed. The neutral pressure in the divertor (a) was feed back controlled. (b) is the line averaged plasma density. The required fuelling rate (c) is about 40% for the reduced cryo-pumping speed. (d) The reduced pumping speed increases the decay time of an impurity puff, in this case argon.

To keep the possibility of operation at higher edge pressures, the cryo-pumping speed can be reduced to 1/3 by using the liquid He by-pass valve. The effect of the reduction of the cryo-pumping speed was demonstrated by a discharge with feed-back controlled divertor neutral

pressure under the roof baffle and using the full and the reduced pumping speed, respectively, as shown in Fig. 8. To achieve the same divertor neutral pressure, the required deuterium gas puff is reduced to about 40% if the liquid He by-pass valve is used to reduce the cryo-pumping speed. A short gas puff, in this case argon, shows the same peak level with and w/o cryo-pump reduction. The latter affects the pump down time only, as can be seen in Fig. 8d.

4.2. Characterization of plasma loaded tungsten

Adiabatically loaded samples offer a wide range of experimental investigations complementary to the investigation of actively cooled samples. It is easy to achieve high surface temperatures to study e.g. effects of W recrystallization and the influence of melt layers on the plasma performance. In addition, the effort to take out adiabatically cooled targets for ex-vessel investigation is low compared to actively cooled targets.

Possible degradation of tungsten due to heat and particle load can be investigated by analysing standard target tiles or by exposing special probes. A first microscopic investigation of shallow cracks as shown in Fig. 9 reveals a bending up on the 10 μm scale. Such protruding peaks might result in melting and material loss due to local overheating. A more detailed investigation is ongoing.

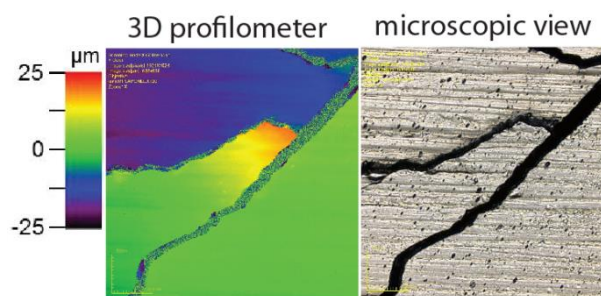


Fig. 9 First analysis of shallow cracks of the target of Fig. 7. The target surface is not smooth anymore. Cracked parts are bending up. The height difference is in the order of a few 10 μm . The area of an image is $638 \times 638 \mu\text{m}^2$

4.3. Dedicated experiments with DIM-II

A main feature of the new divertor is that 2 out of 128 target plates can be exchanged without venting the machine. This is realized by a new divertor manipulator, DIM-II that transports two target tiles including the water cooled support structure out of the divertor region into a target exchange box. DIM-II is designed to be equipped with different front-ends that allow specific physics investigations or divertor component and shaping tests under relevant plasma conditions with a relevant magnetic field and shallow energy and particle impact.

Three general types of front-ends are under discussion, designed or in use. Most simply is to modify standard targets clamped on the support structure to investigate plasma-wall interaction or geometry effects like shadowing or target castellation. These modified targets have already been exposed at the strike line region by DIM-II for a defined set of discharges. Fig. 10 shows 2 types of such sample holders used to expose tungsten and graphite samples for plasma surface investigations.

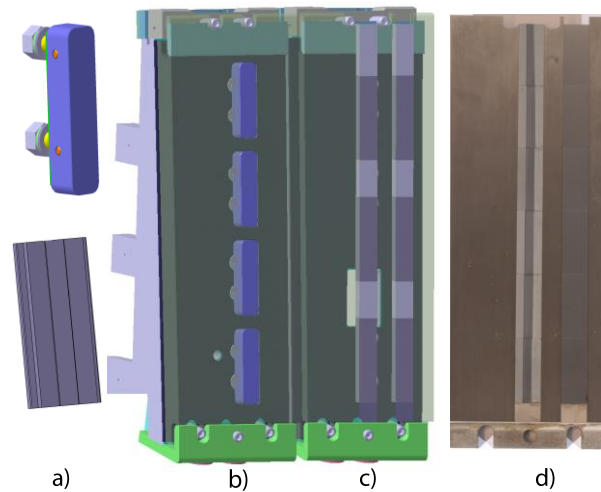


Fig. 10 Standard tungsten targets modified to be sample holders. a) Two types of samples, top: $40 \times 10 \times 10 \text{ mm}^2$ tungsten inlay, bottom: T-shaped graphite inlays $45 \times 10 \times 4 \text{ mm}^3$. b) Sample holder for 10 mm thick tungsten inlays clamped onto the water cooling structure. c) Sample holder for two rows of 4 mm thick inlays. d) Photograph of a sample holder with mounted samples as sketched in c)

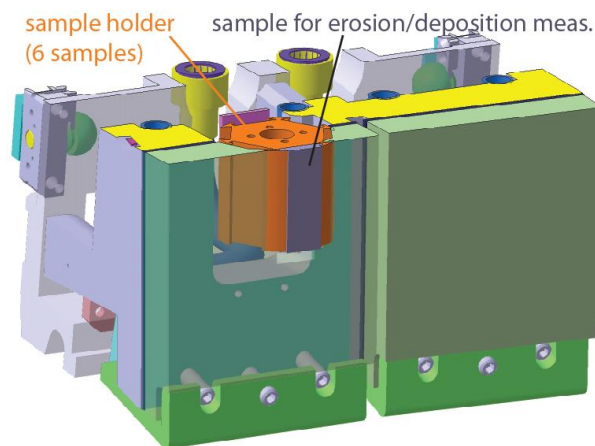


Fig. 11 CAD model of the rotatable sample holder for 6 T-shaped samples. The sample holder will be driven by an external motor. Position control and fixing is realized at the sample holder.

More sophisticated front-ends are under development using a larger space. This can be achieved by integrating the cooling into the probe design and using also the volume of the standard cooling plate for probes getting a volume of about $230 \times 160 \times 80 \text{ mm}^3$. The following front-ends are in discussion and in preparation:

Accepted for publication in Nuclear Fusion

- A rotatable sample holder to allow for shot-resolved measurements as shown in Fig. 11.
- Electrical probes, such as E×B and retarding field analysers that can't be used in discharges with maximum heating power. They have to be exposed on dedicated experiment days.
- Piezo based gas puff valves behind the target for redeposition experiments in combination with spectroscopic measurements.

A contribution to the development of actively cooled targets for future fusion devices can be made by installing actively hot-water cooled targets onto DIM-II and test them under plasma load with ITER relevant magnetic configuration and averaged heat load. A dedicated heat exchanger allows a variation of the applied cooling water temperature between room temperature and 230°C at 4 MPa and covers the expected water temperature range of ITER and a water cooled DEMO. The screening and thermal characterization of such targets will be done in advance in the high heat flux test facility GLADIS [7]. The heat exchanger will be installed in 2015 at ASDEX Upgrade.

5. Summary

In 2013 a solid tungsten divertor, Div-III, was installed in ASDEX Upgrade. It was successfully operated with more than 800 plasma discharges reaching a P_{sep}/R of up to 10 MW/m. First inspection of retrieved tiles revealed cracks attributed to thermal stress induced by the cyclic load. The cracks and post mortem detected melting on a 10 µm scale had no effect on the plasma performance. Leading edges due to a misalignment of divertor modules by disruptions were strongly overloaded, resulting in cracks, recrystallization and melting at the loaded edges w/o effect onto the plasma discharge.

Plasma exposed targets reveals deep cracks through the 15 mm thick target that were not detected at targets after high heat load tests for comparable heat loads.

The accessible collisionality range is extended by increasing the conductance between divertor region and cryo-pump. A liquid He by-pass valve allows operating the cryo-pump with reduced pumping speed to achieve high edge densities.

A new divertor manipulator, DIM-II, allows retracting a relevant part of the divertor into a target exchange box without venting ASDEX Upgrade. Different front-ends can be installed and exposed to the plasma. At present, front-ends for probe exposure, gas puffing, electrical probes and actively cooled prototype targets are under construction or used.

The installation of solid tungsten, the control of the pumping speed and the flexibility for divertor modifications on a weekly base is a unique feature of ASDEX Upgrade and offers together with the extended set of diagnostics the possibility to investigate dedicated questions for a future divertor design.

6. Acknowledgement

This work has been carried out within the framework of the EUROfusion Consortium and has received funding from the European Union's Horizon 2020 research and innovation programme under grant agreement number 633053. The views and opinions expressed herein do not necessarily reflect those of the European Commission.

References

1. Herrmann, A. and (Guest editor), *Special Issue on ASDEX Upgrade*. Fusion Science and Technology, 2003. **44**(3): p. 1-747.
2. Neu, R., et al., *Plasma wall interaction and its implication in an all tungsten divertor tokamak*. Plasma Physics and Controlled Fusion, 2007. **49**(12B): p. B59-B70.
3. Herrmann, A., et al., *Experiences with tungsten coatings in high heat flux tests and under plasma load in ASDEX Upgrade*. Physica Scripta, 2009. **T138**: p. 014059.
4. Herrmann, A., et al., *Design and concept validation of the new solid tungsten divertor for ASDEX Upgrade*. Fusion Engineering and Design, 2013. **88**(6-8): p. 577-580.
5. Herrmann, A., et al., *A solid tungsten divertor for ASDEX Upgrade*. Physica Scripta, 2011. **T145**(T145): p. 014068.
6. Jaksic, N., H. Greuner, and A. Herrmann, *FEM investigation and thermo-mechanic tests of the new solid tungsten divertor tile for ASDEX Upgrade*. Fusion Engineering and Design, 2013. **88**(6-8): p. 1789-1792.
7. Greuner, H., et al., *High heat flux facility GLADIS: Operational characteristics and results of W7-X pre-series target tests*. Journal of Nuclear Materials, 2007. **367-370**: p. 1444-1448.
8. Kallenbach, A., et al., *Partial detachment of high power discharges in ASDEX Upgrade*. IAEA conference 2014, 2014.
9. Huber, A., et al., *Investigation of the impact of transient heat loads applied by laser irradiation on ITER-grade tungsten*. Physica Scripta, 2013. **T159**: p. 197-200.
10. Klimov, N.S., et al., *Experimental study of divertor plasma-facing components damage under a combination of pulsed and quasi-stationary heat loads relevant to expected transient events at ITER*. 2011. p. 014064.
11. Linke, J., et al., *Performance of different tungsten grades under transient thermal loads*. Nuclear Fusion. **51**(7).
12. Mertens, P., et al., *Clamping of solid tungsten components for the bulk W divertor row in JET-precautionary design for a brittle material*. Physica Scripta, 2009. **T138**.
13. Mertens, P., et al., *Bulk tungsten in the JET divertor: Potential influence of the exhaustion of ductility and grain growth on the lifetime*. Journal of Nuclear Materials. **438**: p. S401-S405.

14. Drube, R., et al., *The ASDEX upgrade digital video processing system for real-time machine protection*. Fusion Engineering and Design, 2013. **88**(11): p. 2870-2874.
15. Krieger, K., et al., *Controlled tungsten melting and droplet ejection studies in ASDEX Upgrade*. Physica Scripta, 2011. **T145**.
16. Coenen, J.W., et al., *ELM-induced transient tungsten melting in the JET divertor*. Nuclear Fusion, 2015. **55**(2): p. 23010-23010.